



STRATEGIES

**FOR
FUTURE
CLIMATE
RESEARCH**

STRATEGIES FOR FUTURE CLIMATE RESEARCH^{*)}

Edited by Mojib Latif

^{*)}A collection of papers presented at the birthday colloquium in honour of Klaus Hasselmann's 60th anniversary.

Max-Planck-Institut für Meteorologie
Bundesstraße 55
D-2000 Hamburg 13

CARBONATE BUFFERING OF ANTHROPOGENIC CO₂

By
Ernst Maier-Reimer

Abstract

A three-dimensional model of the oceanic carbon cycle is used to study the potential effects of sediment dissolution on the airborne fraction of man's CO₂ emissions. In accordance with the general agreement that sediment processes are slow, the model predicts almost complete inefficiency on time scales of a century or less. On the thousand year time scale, however, a realistic estimate of the bioturbated sediment pool suggests a reduction of the asymptotic airborne fraction from 15 % to 7 %. The short-term efficiency is not improved when part of the combustion CO₂ is brought directly to the sediment.

1. Introduction

The link between the global climate and the concentration of CO₂ in the atmosphere was already recognised in the last century (cf. Arrhenius, 1896). In view of the increasing anthropogenic emissions of CO₂ from fossil fuel burning, widespread research has been started to investigate in depth the impact of a rise of CO₂. The straightforward approach seemed to be to treat CO₂ as a prescribed external forcing of the climate system. A look into the past, however, clearly reveals that the CO₂ concentration in the atmosphere has undergone substantial variations during the Earth's history (cf. Sundquist 1985). The analysis of air bubbles enclosed in ice cores (Bamola et al. 1985) showed a striking parallelism between CO₂ concentration in the atmosphere and the local temperature as deduced from the hydrogen isotopes. The fast change of atmospheric CO₂ by 80 ppm within a very few thousand years poses a major concern for ongoing geochemical research. Up to now, no satisfactory explanation has been given of how this change could be achieved from plausible alterations of the global carbon cycle (cf. Heinze et al., 1991). However, it is now generally accepted that the carbon cycle represents an important intrinsic component of the climate system, and that when studying the effects of the emission of fossil fuel CO₂ we have to examine carefully the potential feedback of this component.

The role of biological processes in the uptake of fossil fuel CO₂ by the ocean is often misinterpreted. The naive sketch that the excess CO₂ in the atmosphere is brought into the depth of the ocean by the biological pump is in striking contradiction to the fact that the CO₂-content of the atmosphere has remained almost perfectly constant during the last ten thousand years before the onset of anthropogenic emissions. The natural biological pumps are in equilibrium with the upwelling of remineralized nutrients. In regions of high productivity, the CO₂-content of the surface water is depleted by only 15 % of the deep sea value. It is hard to imagine that an increase of 10 % (the increase that would be in equilibrium with a doubling in the atmosphere (cf. Revelle and Suess, 1957)) could substantially improve the utilization of nutrients. The strength of the gradients of dissolved CO₂ in the ocean, however, is due primarily to the biological processes; thermodynamical effects alone could explain only one fifth of the observed gradients. Without the biological pumps, the ocean would chemically be quite different from today's real ocean even in the abiotic components. A direct effect of the biological pump on the uptake of CO₂ can be expected only from changes in the pumping mechanisms. Such changes could result in a modified thermodynamic field through changes in the plankton communities or through a changed residence time of particulate matter in the deep ocean (cf. Heinze et al., 1991).

An indirect effect of biology on the uptake of fossil fuel CO₂ is provided by the existence of sediment layers of which the upper ten or twenty centimeters are bioturbated and, thus, still in close contact with the overlying water. Incidentally, this pool is estimated to contain the same amount of carbon as the present estimates of coal resources (Broecker and Takahashi, 1977). During the uptake of excess CO₂ the surface water becomes more acid. When it reaches the sediment layer, it tends to dissolve the sediment and, consequently, to neutralize the acidification as well as the excess pCO₂. In the modern ocean, carbonate sediments are preserved - in the global average - at depths shallower than 4 km. In equilibrium with a doubled CO₂ content in the atmosphere, the concentration of CO₃⁻ ions in the seawater will be halved and the preservation level ("lysocline") will rise by several kilometers (cf. Fig.1) and thus expose the corresponding sediment layers to dissolution.

In this paper, I discuss two experiments with the Scripps Hamburg Model of the Oceanic Carbon Cycle (SHMOCC). Section II gives a short description of the model. In section III the short-term efficiency of the sediment dissolution is discussed for emission scenarios for the next century; one of the scenarios assumes a release of one third of the emission into the

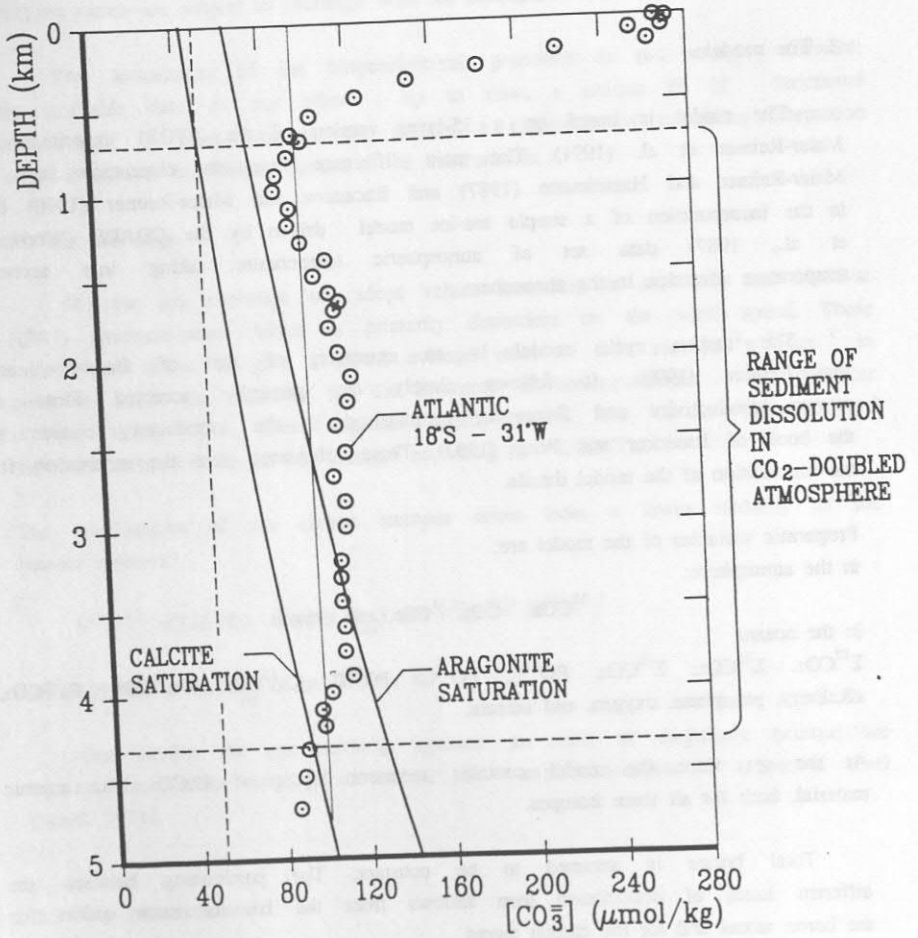


Fig.1 Solubility products of $CaCO_3$ and CO_3^{2-} at a station in the southern Atlantic (after Broecker and Peng, 1982).

Gibraltar strait.

2. The model

The model is based on a 15-layer version of the ATOS1 experiment of Maier-Reimer et al. (1991). The main difference from the circulation field of Maier-Reimer and Hasselmann (1987) and Bacastow and Maier-Reimer (1990) lies in the incorporation of a simple sea-ice model driven by the COADS (Woodruff et al., 1987) data set of atmospheric temperature taking into account temperature advection in the atmosphere.

The carbon cycle model is an extension of that of Bacastow and Maier-Reimer (1990). It follows closely the generally accepted ideas of primary productivity and fluxes as summarized in the introductory chapter in the book of Broecker and Peng (1983). These references give the motivation for the formulation of the model details.

Prognostic variables of the model are:
in the atmosphere:

$$^{12}\text{CO}_2, ^{13}\text{CO}_2, ^{14}\text{CO}_2, \text{ and oxygen}$$

in the ocean:

$$\Sigma^{12}\text{CO}_2, \Sigma^{13}\text{CO}_2, \Sigma^{14}\text{CO}_2, \text{PO}^{12}\text{C}, \text{PO}^{13}\text{C}, \text{PO}^{14}\text{C}, \text{Ca}^{12}\text{CO}_3, \text{Ca}^{13}\text{CO}_3, \text{Ca}^{14}\text{CO}_3, \\ \text{alkalinity, phosphate, oxygen, and silicate.}$$

At the sea floor the model contains sediment layers of CaCO_3 and organic material, both for all three isotopes.

Total borate is assumed to be constant; The partitioning between the different states of dissociation then follows from the law of mass action for the boron atoms and for the carbon atoms.

Formally, the model is characterized by a set of differential equations:

$$\frac{\partial C_i}{\partial t} + \underline{V} \cdot \nabla C_i + D C_i = \lambda_i C_i + \sum_k F_{ik} (C_i, C_k)$$

where C_i stands for any of the tracers, \underline{V} is the vector of the advection velocity, D denotes the diffusion operator, λ denotes tracer specific sink/source terms like decay of ^{14}C , and F denotes the nonlinear interaction functionals between the tracers. As boundary condition we impose zero fluxes

across all boundaries for all tracers, except for oxygen and the carbon isotopes which are subject to exchange with the atmospheric variables.

The formulation of the biogeochemical processes is not straight-forward; the available data do not allow, up to now, a unique fit of functional relationships. In most processes we assume a parameter of maximum interaction which is reduced by limiting factors of the environment.

2.1 Gas exchange

For the gas exchange we adopt values according to the Liss and Merlivat (1987) parametrization which is primarily dependent on the wind speed. These values were scaled to give a global average value of $0.06 \text{ mol m}^{-2} \text{ y}^{-1} \text{ ppm}^{-1}$ in order to match the estimates for the inventory of bomb-produced ^{14}C (Broecker et al., 1985). With these regional coefficients λ , the air-sea difference of the CO_2 partial pressure ΔPCO_2 changes according to $-\lambda \Delta\text{PCO}_2$.

The fractionation of the carbon isotopes stems from a lower mobility of the heavier isotopes:

$$F^{13}/F^{12} = (1.02389 - 9.483/T_{\text{abs}}) \text{ and } F^{14}/F^{12} = (F^{13}/F^{12})^2$$

(Mook, 1986), where T_{abs} is the SST in K.

For oxygen the gas exchange operates an order of magnitude quicker; we assume the surface oxygen to be at the temperature-dependent saturation level (Weiß, 1973).

2.2 New production:

Depending on the phosphate concentration, the new production of soft tissue material is written:

$$\text{NP} = r P (P/(P + P_0))$$

assuming a higher remineralization rate in nutrient-poor water. r depends on the temperature T (in Celsius), the solar angle Δ , and the actual depth of the mixed layer as represented in the model by the depth C_d of the convective column:

$$r = r_0 \cos \Delta (50m/ Cd) (T+2)/(T+10).$$

We did not assume any kind of iron limitation as proposed by several authors (e.g. Martin et al., 1990).

NP effects a transformation from P and ΣCO_2 to the POC (Particulate Organic Carbon) pools. The alkalinity is increased by 16 NP due to the incorporation of nitrate into soft tissue. The implementation of heavy carbon isotopes is proportional to 0.98 and 0.9604 times the local isotopic ratios of ^{13}C and ^{14}C , respectively, in ΣCO_2 . These newly formed POC quantities are released in the depth z according a penetration flux $(z/100m)^{-0.8}$ for $z > 100m$ (Suess, 1980, Berger, 1987). The flux reaching the bottom is added to an organic sediment layer where remineralization occurs with a time constant of 0.1/month. In the experiments described here, the organic sediment pool is less than 15 Gigatons; for the global carbon budget it is meaningless. The PCO_2 of the surface ocean reacts very sensitively on the details of the production. A detailed discussion will be given in (Kurz and Maier-Reimer, in prep.). The optimal productivity r_0 was tuned to simulate a realistic pattern of surface phosphate (cf. fig.2).

2.3 Remineralization:

Provided there is enough oxygen, we parameterize remineralization by a time constant of 50 months. During this process oxygen and alkalinity are reduced according to the relative Redfield ratios. The remineralized POC is added to the local concentrations of alkalinity, phosphate, and ΣCO_2 in all three isotopes. We do not consider processes like denitrification or sulfate transformation to H_2S . The resulting distribution of POC gives an indication of where these processes could take place. Nor do we consider the crystallization of apatite which could happen in concentrations of more than $3 \mu mol/kg$ of phosphate (Atlas and Pytkowicz, 1977).

2.4 Shell material

We assume silicate to be the preferred concrete to build shells. The redissolution of silicate is weaker than that of carbonate. Thus, the export of silicate shells is connected with the gross primary productivity rather than with the new production, the main process of our model. With a (rather arbitrarily chosen) constant relation of 1:10 between new and gross production

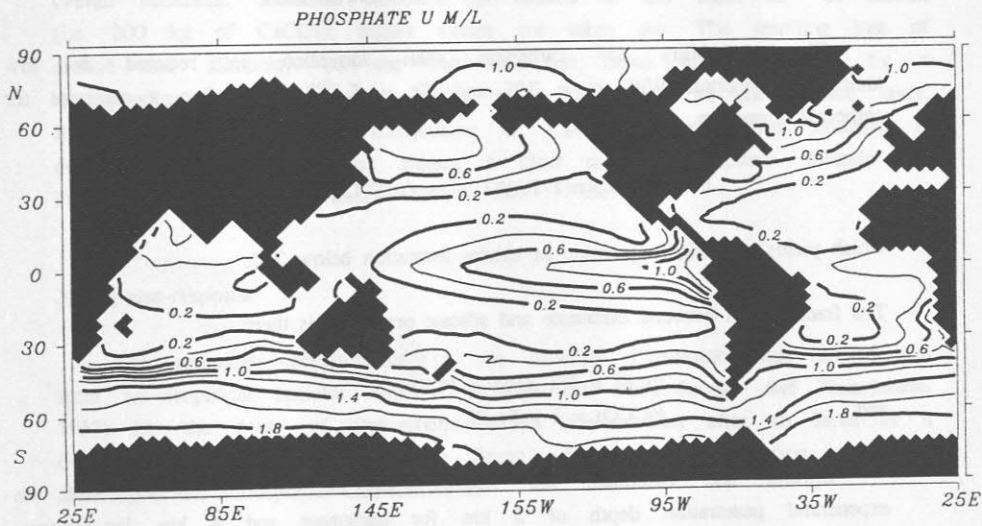


Fig.2 Simulated surface phosphate concentration for January

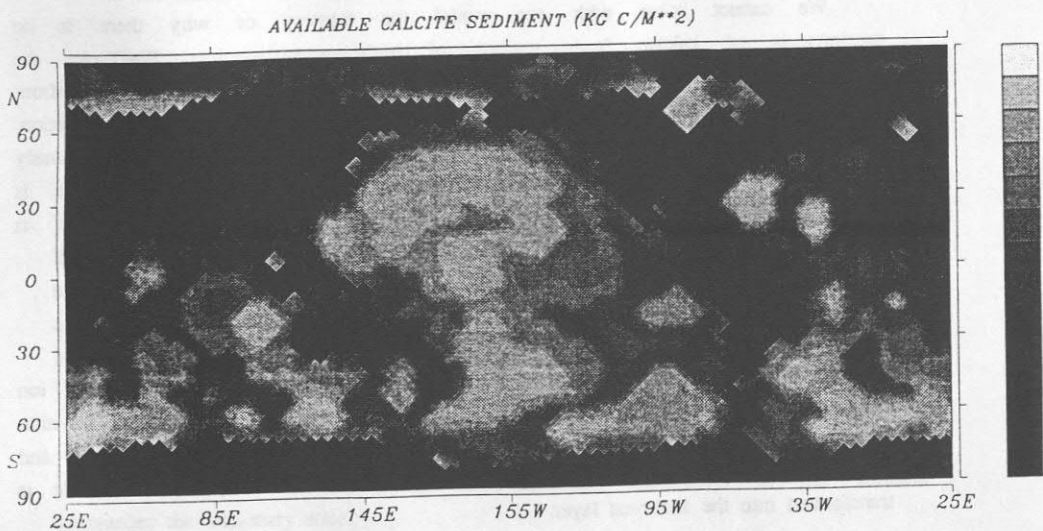


Fig.3 Simulated bioturbated calcite sediment

we define a potential for silicate production $PSi = Si/(Si+Si_0)$.

The probability for carbonate shell formation is reduced in low temperature regions. With $\alpha = 3/K$ and $T_c = 5^\circ C$, we define a potential for carbonate formation

$$PCO_3 = \exp(\alpha(T-T_c))/(1 + \exp(\alpha(T-T_c)))$$

which yields a strong suppression of calcite formation below $2^\circ C$.

The fractionation between carbonate and silicate producers is then:

$$Fr Si = PSi / (PSi + PCO_3)$$

and

$$Fr CO_3 = 1 - Fr Si.$$

Silicate and carbonate are released to the interior ocean with an exponential penetration depth of 2 km for carbonate and 4 km for silicate. During the formation of carbonate shells there is no fractionation between carbon isotopes.

2.5 Sediment of Calcium-Carbonate

We cannot solve with our model the mystery of why there is no precipitation of calcite from regions of high supersaturation. We take the solubility product to be dependent on salinity, temperature, and pressure from Broecker and Takahashi (1978) and we compute locally the degree of saturation. We assume that the equilibrium is established as a result from continuously acting crystallization and dissolution processes in which the recombination is somehow blocked. In supersaturated water, the monthly dissolution is parameterized by

$$1 - \Delta CO_3 / (|\Delta CO_3| + \Delta CO_{30}),$$

with $\Delta CO_{30} = 10^{-4}$ mol/kg, where ΔCO_3 is the excess carbonate ion concentration. In undersaturated water we assume complete dissolution within one month. Spontaneous crystallization is zero in the interior ocean and 0.2/month in the bottom layers of the model. Here, the newly formed calcite is transformed into the sediment layer.

The sediment layer represents only the bioturbated upper 10 cm of the

overall sediment. Sediment thickness is limited at 2.5 kmol m^{-2} of carbon (i.e. 200 kg of CaCO_3); higher values are taken out. The resulting loss of carbon and alkalinity (in the run described here) is compensated by a corresponding amount of river inflow along the coasts in the surface layer. Fig.3 shows the resulting distribution of CaCO_3 sediment. The structure is dominated by the midoceanic ridges; a clear distinction between Atlantic and Pacific, however, is clearly seen.

3. Impulse-response

The essential characteristics of the model's CO_2 -uptake can be derived from an empirical impulse response function (cf. Maier-Reimer and Hasselmann, 1987) i.e. the decay of atmospheric excess concentration after an input of a δ -function type. Fig.4 compares the Green's functions resulting from a sudden doubling of the atmospheric CO_2 -content for

- 1) an inorganic carbon cycle model (like Maier-Reimer and Hasselmann, 1987, but based on the more realistic circulation)
- 2) a sediment-free biotic model (like Bacastow and Maier-Reimer, 1990)
- 3) the model with a stationary (preindustrial) sediment pool of 5800 Gt
- 4) the outcrop-diffusion model (Siegenthaler, 1983) with the calibration of the transport rates by bomb ^{14}C .

The close agreement between 1) and 2) is, of course, a consequence of the assumption of nutrient limitation in the biological production. Slight differences may be attributed to the fact that, after calibration to the same atmospheric CO_2 -content, the model versions exhibit different patterns of $\Delta p\text{CO}_2$ between ocean and atmosphere (cf. Maier-Reimer and Hasselmann, 1987). The experiment with the included sediment starts with the same slope as 1) and 2). Only after a few centuries, when the alkalinity released during the sediment dissolution in the northern Atlantic reaches the convection areas around Antarctica, does the line start to lie substantially below the other two lines.

For these experiments, the model as described in the previous sections was run with the annual mean circulation field and with a time step of one year. This allows for an increasingly economic integration as the solution approaches the stationary state.

It must be noted that, due to many nonlinearities in the system, the

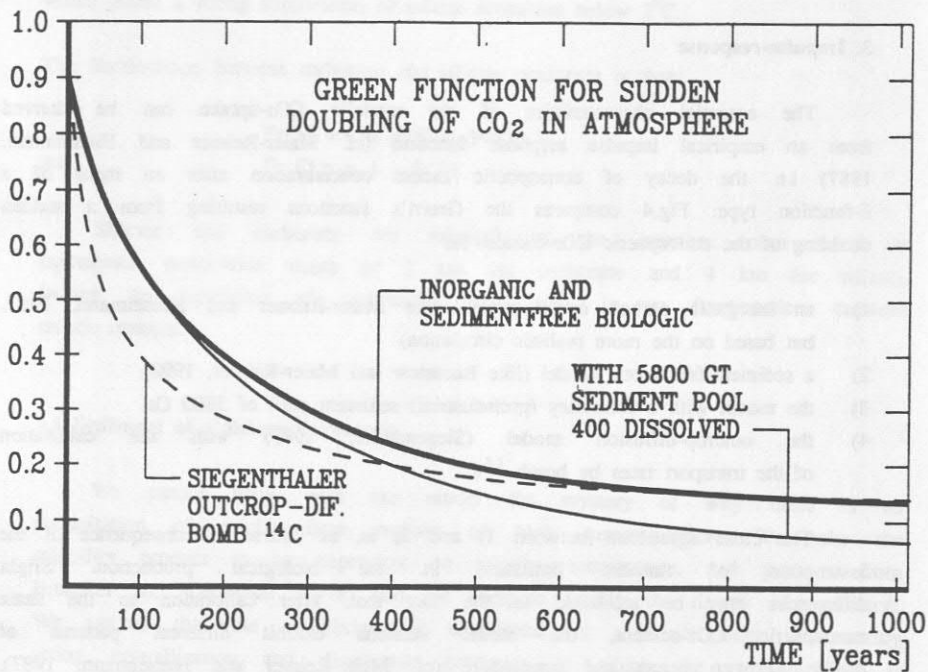


Fig.4 Simulated "empirical" impulse response Green's function for different models

annual mean state of the seasonal model - which is used for the transient runs - need not necessarily coincide exactly with the state of the annual mean model; however, for the slow changes of stationary states as described by the Green's functions, almost identical answers of both model versions are expected.

The figure also displays the response of the outcrop-diffusion model after calibration with bomb- ^{14}C (Siegenthaler, 1983). It is shown in that paper that the outcrop-diffusion model generally predicts a faster uptake of CO_2 than the traditional box-diffusion model, (Oeschger et al., 1975) and that the calibration with bomb- ^{14}C provides a faster uptake than the calibration with natural radiocarbon. The line for box-diffusion model, when calibrated with natural ^{14}C , would lie rather close to the lines 1) and 2).

4. Fossil fuel emissions

For the preindustrial state, the alkalinity inventory was calibrated to produce a stationary CO_2 -concentration of 278 ppm in the model atmosphere. Starting from the year 1750, the model was spun up to a modern state - representative of the year 1988 - by prescription of the observed values taken from the Siple ice core (Staffelbach et al., 1991) up to 1957 and, after that year, the annual mean values of the Mauna Loa observatory (Keeling, 1989). During the last year of this period, the DIC content of the ocean increased by 1.58 Gt, of which 1.54 Gt came from the atmosphere and 0.04 came from already initialized sediment dissolution. The atmospheric increase of that year was 3.92 Gt. The sum of both components adds up to 5.46 Gt, whereas the industrial production was 5.8 Gt. This means that, neglecting all effects of the terrestrial biosphere, there is a missing sink of the cumulative input from fossil fuel burning and from cement manufacture of 0.3 Gt which cannot be explained by the model. Fig. 5 displays the increase of alkalinity and DIC for the time span 1750-1988 along a section in the western Atlantic. The DIC increase exhibits a pattern very similar to the reconstruction of the bomb ^{14}C : in the subtropical gyres the increase by appr. $50 \mu\text{mol/l}$ (2.5 % of the undisturbed value) is nearly in equilibrium with the atmospheric increase of 25 %; a penetration into the deep ocean is seen primarily in the northern Atlantic, whereas around Antarctica the signal is more diluted by the strong mixing in that region. The change of alkalinity starts from the Iceland sill where thick sediment is in closest connection to the atmosphere and, thus, to the anthropogenic perturbation. For the atmospheric CO_2 , however, this small amount of released alkalinity is still meaningless. Fig.6 shows the net flux

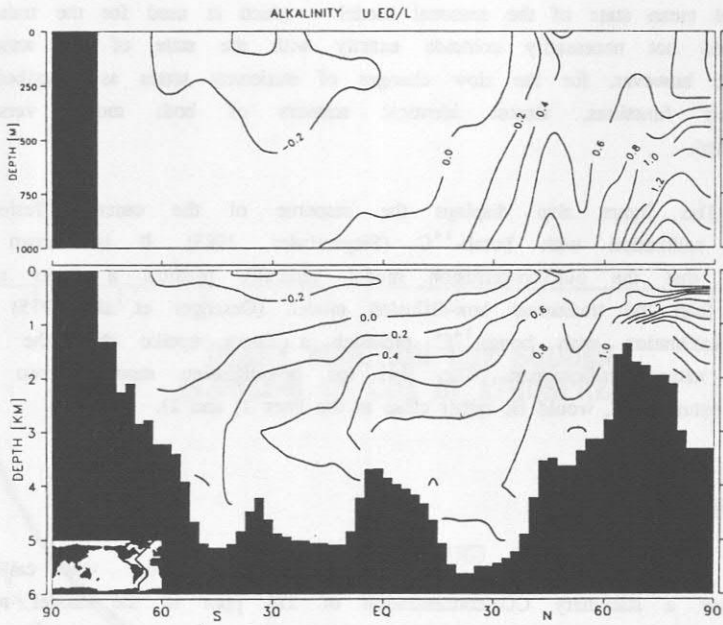


Fig.5a Change of alkalinity by sediment dissolution 1750 - 1988

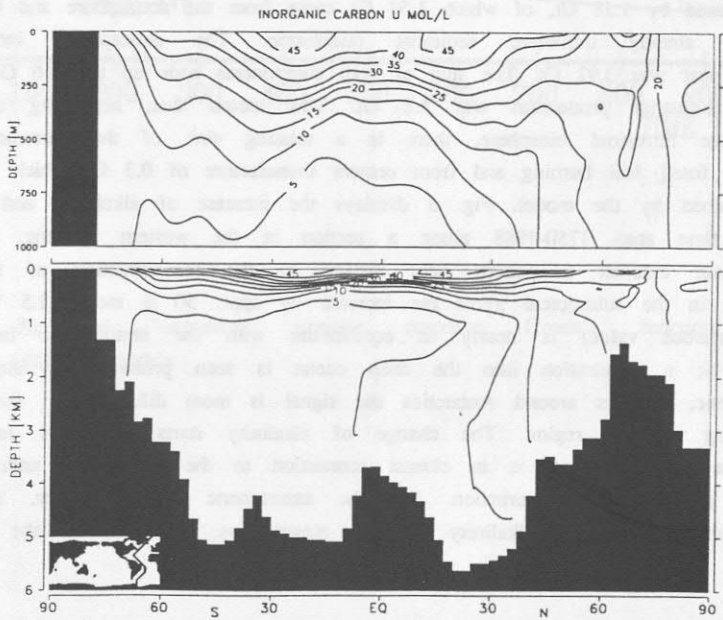


Fig.5b Change of dissolved inorganic carbon 1750 - 1988

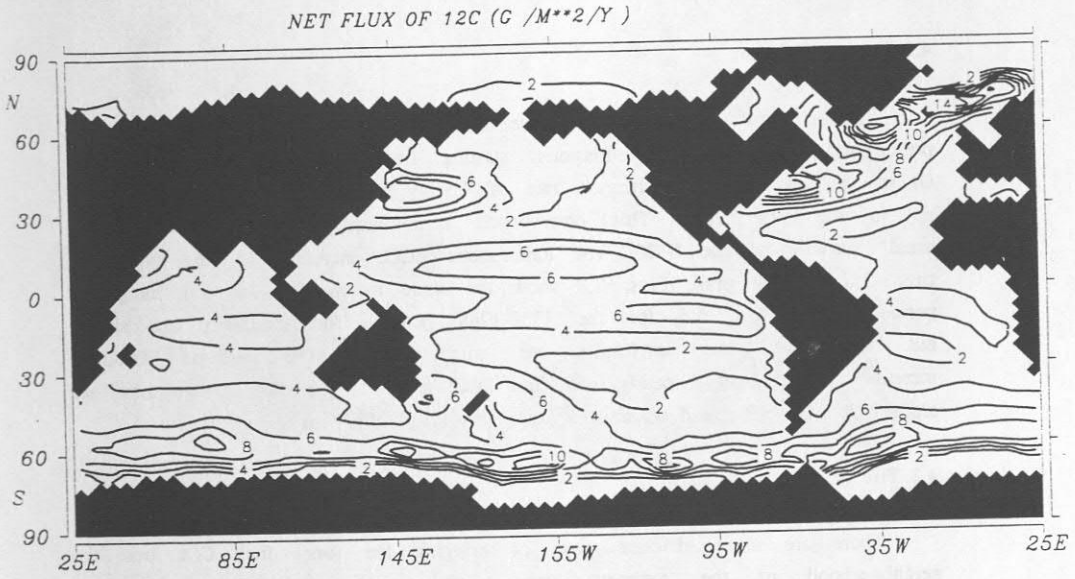


Fig.6 Change of net flux of CO_2 into the ocean 1750 - 1988

of anthropogenic CO₂ into the ocean. This figure represents the difference of the fluxes between 1988 and 1750. The apparent downward flux in the equatorial oceans is an artefact resulting from the reduction of the outgassing in those regions.

4.1 Future emission

Starting from this 1988 state, the experiment was continued by prescription of fossil fuel emissions: starting from the real emission of 5.7 Gt in the year 1988, an increase rate of 1.5%/y was assumed for the emissions up to the year 2100. This corresponds approximately to the "business as usual" scenario of the IPCC. The atmospheric pCO₂ increased in this experiment from 352 to 968 ppm. Figs. 7,8 show the same information for this integration period as do figs. 5,6 for the 1750-1988 period. The structures are similar but, of course, the amplitudes are much higher. The released alkalinity increased approximately linearly with the DIC; even at the surface, we now see a local increase of 3 μ eq/l which still has a very small effect on the pCO₂.

4.2 The Marchetti Scenario

There are more efficient ways of bringing the fossil fuel CO₂ into the neighbourhood of the sediment layer. Some years ago it was proposed (Marchetti, 1977) to remove a substantial fraction of the fossil fuel emissions from power plants - which actually contribute approximately one third to the total emission - and to release it in a suitable aggregate into the deep sea. As a promising place, he identified the Gibraltar strait, where the salty Mediterranean water spreads rather quickly from a sill depth of 300 m into the deep Atlantic.

The classical map of this Mediterranean salty tongue (Wüst, 1935) clearly shows that there is a northern branch going up to the Iceland sill where it can reach the region of deep water formation. It has been speculated (Käse, pers. comm.) that this combination of salty water and cool atmosphere should play a major role in the effective formation of NADW. When CO₂-enriched water approaches this region along the bottom, the upward mixing by convection will be counteracted by the large scale downward motion of the NADW.

For a simulation of the Marchetti scenario, one third of the total production - starting in 1989 - was released into two gridpoints in the Atlantic near the Spanish coast. For the year 2100, this experiment predicts an atmospheric CO₂-content of 749 ppm, i.e. an increase of slightly less than

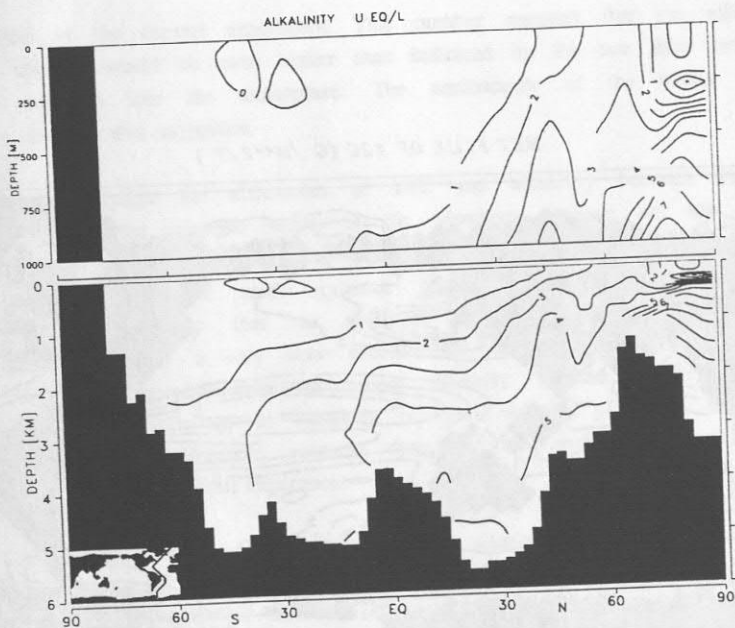


Fig. 7a Change of alkalinity by sediment dissolution 1989 - 2100

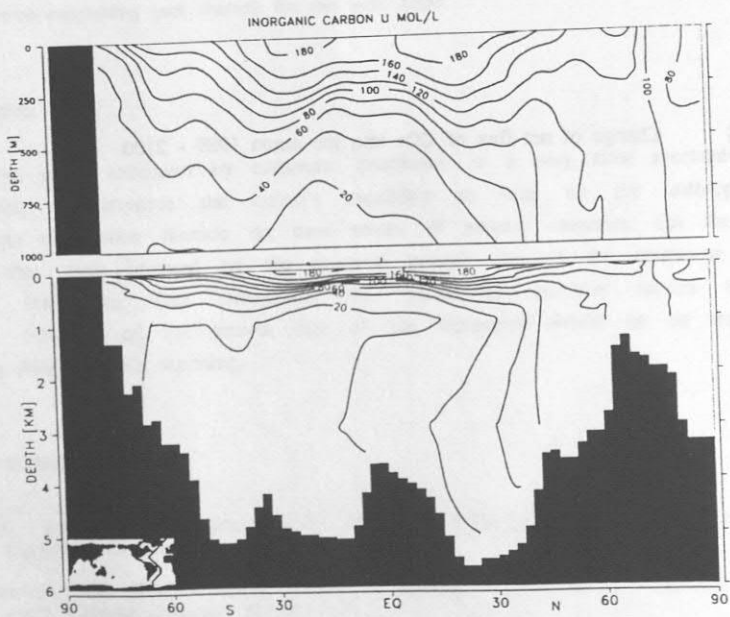


Fig. 7b Change of dissolved inorganic carbon 1989 - 2100

NET FLUX OF ^{12}C ($\text{G} / \text{M}^2 / \text{Y}$)

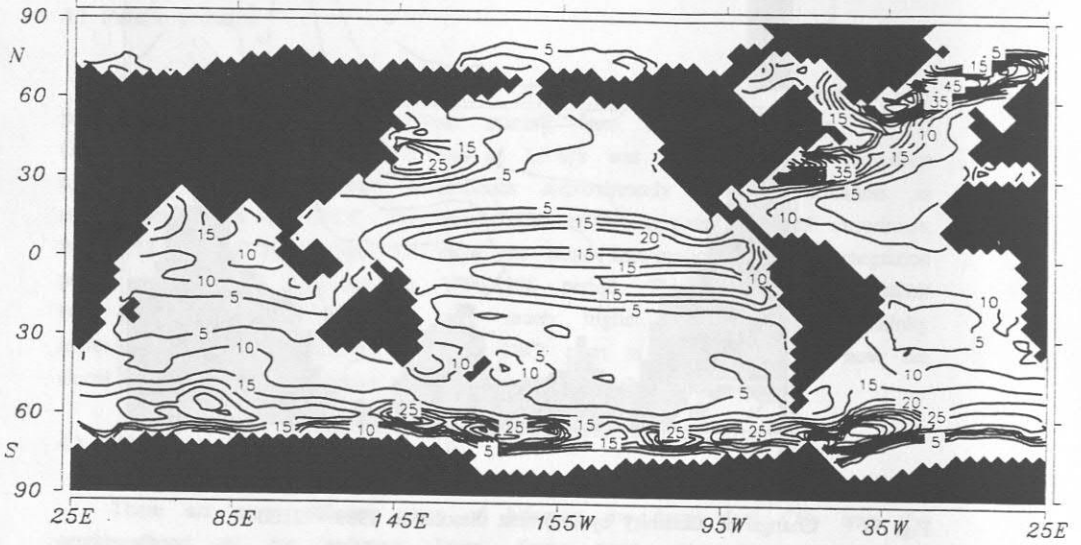


Fig.8 Change of net flux of CO_2 into the ocean 1989 - 2100

two thirds of the control experiment. This number suggests that the efficiency of the scenario would be even higher than indicated by the one third reduction of the emission into the atmosphere. The nonlinearity of the buffer factor, however, devalues this suggestion.

Fig. 9 displays the differences of DIC and alkalinity between the two experiments. As the injection points of the Marchetti scenario are not located on the section, the obvious maximum of the signal is at a quite different latitude according to the rather cyclonic circulation in the 2 km horizon. Here again, it is seen that the sediment dissolution of the model is - probably realistically - a very slow process; the excess plume of DIC has a much higher concentration than the excess alkalinity. In the southern part of the Atlantic, the difference in alkalinity is even reversed. Due to the lower acidification in the Marchetti scenario there is less sediment dissolution in that region than in the control experiment.

The combined effect of the differences of alkalinity and DIC on the CO₂ uptake by the ocean is demonstrated in fig. 10 which displays the difference in the air-sea flux between the two experiments. In the subtropical gyres, the difference is less than 1 g C m⁻²y⁻¹. In the regions of deepwater formation in the southern ocean, the difference reaches 10 g C m⁻²y⁻¹. Around Iceland, the difference exceeds 50 g C m⁻²y⁻¹. Here, the Marchetti scenario even provides an effective outgassing (not shown) for the year 2100.

Conclusion

The pCO₂ reduction by carbonate dissolution is a very slow mechanism. It will help to improve the ocean's capability to take up the anthropogenic emissions of carbon dioxide on time scales of several centuries. On the sixty years time scale imposed by the assumed growth rate of the emissions, it is almost ineffective. This strengthens the results of previous studies that a drastic reduction of the growth rate of the emissions would be an important step to delay the CO₂ warming.

REFERENCES:

- Atlas, E. and R.M. Pytkowicz, 1977: Solubility behavior of apatite in seawater. *Limnology Oceanography* 22, 290-300.
- Bacastow, R. and E. Maier-Reimer, 1990: Circulation model of the oceanic carbon cycle. *Climate Dynamics* 4, 95 - 125

ALKALINITY U EQ/L

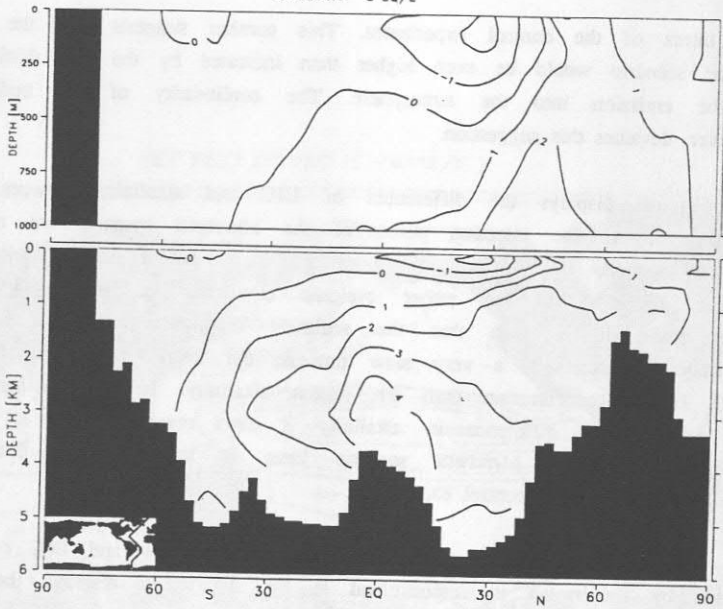


Fig.9a Difference of dissolved alkalinity between the Marchetti scenario and the control experiment in 2100

INORGANIC CARBON U MOL/L

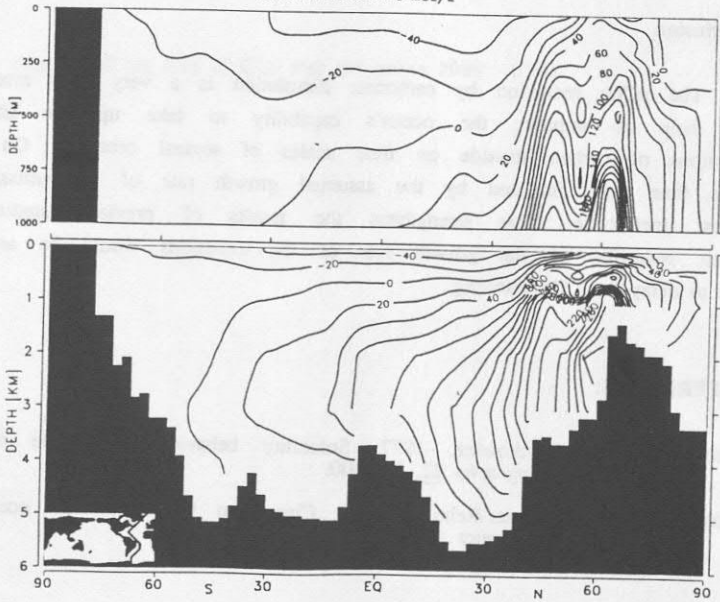


Fig.9b Difference of dissolved inorganic carbon between the Marchetti scenario and the control experiment in 2100

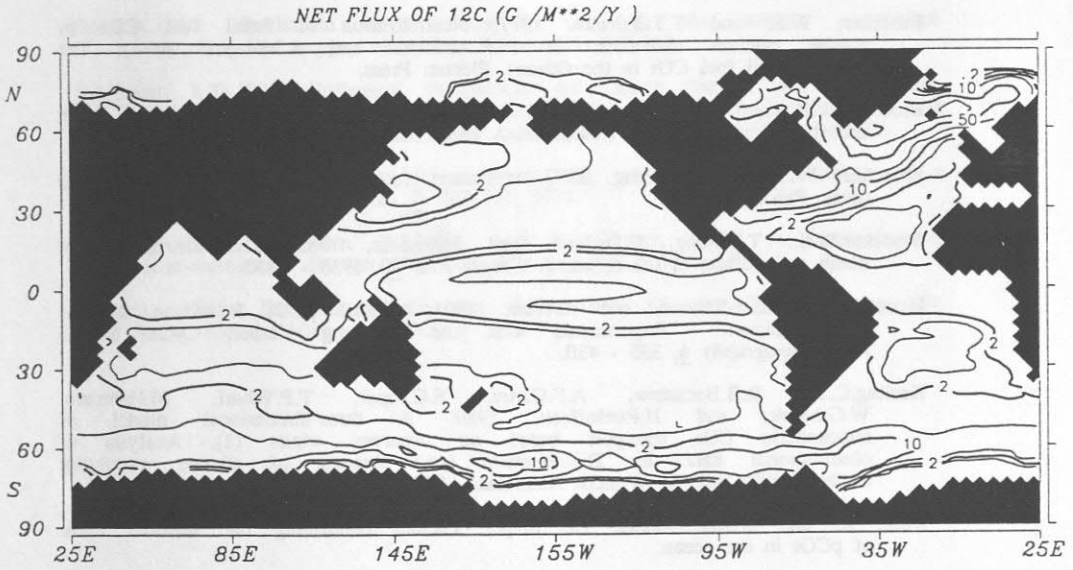


Fig.10 Difference of the net flux of CO₂ into the ocean between the Marchetti scenario and the control experiment in 2100

- Barnola, J.M., D. Raynaud, Y.S. Korotkevich, and C. Lorius, 1987: Vostok ice core provides 160,000-year record of atmospheric CO₂. *Nature* 329, 408 - 414
- Berger, W.H., K. Fischer, C. Lai, G. Wu, 1987: Ocean Productivity and organic carbon flux. SIO Ref. 87-30.
- Broecker, W.S. and T. Takahashi, 1977: Neutralization of fossil fuel CO₂ by marine calcium carbonate. in: N.R. Andersen and A. Malahoff (eds.): The fate of fossil fuel CO₂ in the Oceans. Plenum Press.
- Broecker, W.S. and T. Takahashi, 1978: The relationship between lysocline depth and in situ carbonate ion concentration. *Deep Sea Research* 25, 65-95.
- Broecker, W.S. and T.H. Peng, 1982: Tracers in the Sea, 691 pp. Eldigio press, Palisades.
- Broecker, W.S., T.H. Peng, G. Östlund, and M. Stuiver, 1985: The distribution of bomb radiocarbon in the ocean. *J. Geoph. Res.* 90, 6953 - 6970
- Heinze, C., E. Maier-Reimer, and K. Winn, 1991: Glacial pCO₂ Reduction by the World Ocean - Experiments with the Hamburg Carbon Cycle Model. *Paleoceanography* 6, 395 - 430.
- Keeling, C.D., R.B. Bacastow, A.F. Carter, S.C. Piper, T.P. Whorf, M. Heimann, W.G. Mook, and H. Roeloffzen, 1989: A three-dimensional model of atmospheric CO₂ transport based on observed winds (1). Analysis of observational data. in: D.H. Peterson (ed.) Aspects of climate variability in the Pacific and the Western Americas. AGU monograph 55.
- Kurz, K. and E. Maier-Reimer (in prep.): Factors controlling the seasonal cycle of pCO₂ in the ocean.
- Martin, J.H., S.E. Fitzwater, and R.M. Gordon, 1990: Iron deficiency limits phytoplankton growth in Antarctic waters. *Global Biogeochem. Cycles* 4, 5-12
- Liss, P.S. and L. Merlivat, 1986: Air-Sea gas exchange rates: Introduction and Synthesis. in: P. Buat-Menard (ed) The Role of Air-Sea Exchange in Geochemical Cycling. D. Reidel, pp 113-127.
- Maier-Reimer, E., U. Mikolajewicz, and K. Hasselmann, 1991: On the sensitivity of the global ocean circulation to surface forcing. *J. Phys. Oceanogr.* submitted.
- Maier-Reimer, E. and K. Hasselmann, 1987: Transport and storage of CO₂ in the ocean - an inorganic ocean-circulation carbon cycle model. *Climate Dynamics* 2, 63-90.
- Marchetti, C., 1977: On geoengineering and the CO₂ problem. *Climatic Change* 1, 59-68, 1977
- Mook, W.G., J.C. Bommerson, and W.H. Staverman, 1974: Carbon isotope fractionation between dissolved bicarbonate and gaseous carbon dioxide. *Earth and Planetary Science letters*, 22, 169 - 176.
- Oeschger, H., U. Siegenthaler, U. Schotterer, and A. Gugelmann, 1975: A box diffusion model to study the carbon dioxide exchange in nature. *Tellus* 27, 168-192.

- Revelle, R. and H.E. Suess, 1957: Carbon dioxide exchange between atmosphere and ocean and the question of an increase of atmospheric CO₂ during the past decades. *Tellus* 9, 18-27.
- Siegenthaler, U., 1983: Uptake of Excess CO₂ by an Outcrop - Diffusion Model of the Ocean. *J. Geophys. Res.* 88, C6, 3599- 3608.
- Suess, E., 1980: Particulate organic carbon flux in the oceans - surface productivity and oxygen utilization. *Nature* 288, 260-263.
- Sundquist, E.T., 1985: Geological Perspectives on Carbon Dioxide and the Carbon Cycle. In : E.T. Sundquist and W.S. Broecker (eds.): *The Carbon Cycle and Atmospheric CO₂: Natural Variations Archean to Present*. AGU Monograph 32.
- Weiss, R.F., 1974: Carbon Dioxide in water and sea water: the solubility of a nonideal gas. *Marine Chem.* 2, 203-215, 1974.
- Woodruff, S.D., R.J. Slutz, R.J. Jenne, and P.M. Steurer, 1987: A comprehensive ocean-atmosphere data set. *Bull. Am. Met. Soc.* 68, 1239 - 1250.
- Wüst, G., 1935: Die Stratosphäre des Atlantischen Ozeans. *Wiss. Ergebn. Dt. Atlant. Exped. "Meteor" 1925-27* 6